EFDA–JET–PR(00)02

Spectroscopy of Hydrocarbon Fluxes in the JET Divertor

M F Stamp et al

EFDA EUROPEAN FUSION DEVELOPMENT AGREEMENT
JET

EFDA–JET–PR(00)02

Spectroscopy of Hydrocarbon Fluxes in the JET Divertor

M F Stamp, S K Erents, W Fundamenski,
G F Matthews, R D Monk[1].

EURATOM/UKAEA Fusion Association, Culham Science Centre, Abingdon,
Oxfordshire, OX14 3DB, UK.
[1]Max Planck Institut für Plasmaphysik, Boltzmannstrasse 2, 85748 Garching, Germany.

Preprint of a Paper to be submitted for publication in Physics Scripta

October 2000

ABSTRACT

The injection of hydrocarbons into the JET Gas Box divertor in ohmic and L-mode discharges has been used to calibrate the intrinsic hydrocarbon erosion yields and to determine the variation of the photon efficiency with the edge ion flux. Methane erosion yields of 5% for CD_4 and 3% for CH_4 were measured, with no sign of any flux dependence. The erosion yield of ethane/ ethene was lower but increased with the edge ion flux (increasing edge plasma density, decreasing edge electron temperature) such that it dominated the molecular carbon source at high density. The methane and ethane photon efficiencies (the number of molecular dissociations per emitted photon) were both not constant, but were found to increase with increasing density (increasing edge ion flux, decreasing edge electron temperature).

1. INTRODUCTION

Graphite is a candidate material for the walls and divertor of a fusion reactor because of its low Z and good thermal and mechanical properties. Its major drawbacks are the high erosion rate from chemical sputtering and the tritium inventory in redeposited carbon films [1]. Recent in-situ erosion measurements [2-4] have indicated a promising trend of reduced erosion yields at high incident particle fluxes, offering the hope that at the high fluxes expected in reactor-grade divertors chemical erosion and redeposition will be mitigated. However, these studies assumed a constant photon efficiency (D/XB, the number of molecular dissociations per emitted photon) for their determination of the methane flux from spectroscopic observation of the CD molecular band at 431nm.

We have investigated the behaviour of the hydrocarbon erosion yield in the JET Gas Box divertor with a series of dedicated experiments in which methane (CD_4 and CH_4) and ethene/ethane (C_2H_4, C_2H_6) hydrocarbons were puffed from the divertor gas introduction modules (GIMs) into either deuterium or hydrogen plasmas. Ohmic and L-mode (2MW NBI) 2.4MA, 2.5T vertical target X-point plasmas were mainly used for this study. The typical magnetic configuration is shown in fig.1, which also shows the locations of the divertor Langmuir probes and some spectroscopic lines-of-sight. Light collected from the integral inner and outer divertor views was routinely monitored by the KS3 survey

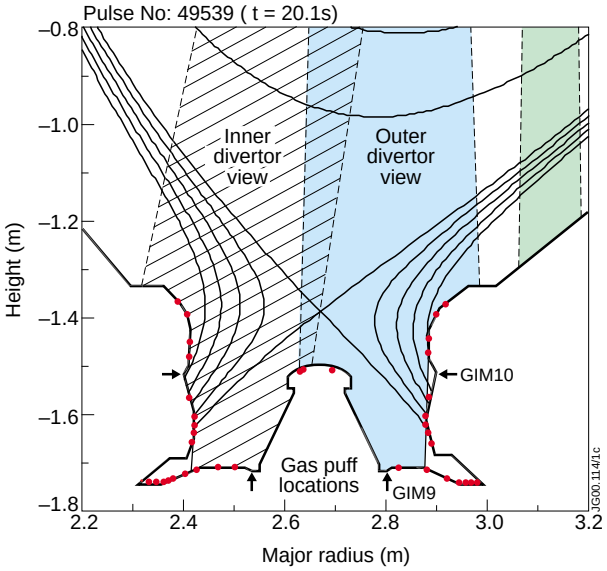

Fig.1: The magnetic configuration of the discharges used, showing the fixed Langmuir probe positions (solid dots) and the lines-of-sight (los) of the visible spectroscopy. The inner and outer divertor los are the integral over the hatched and shaded areas indicated.

spectrometer, which clearly showed CD (from break-up of CD_4) and C_2 (from break-up of C_xD_y, x>1) molecular band features (fig.2).

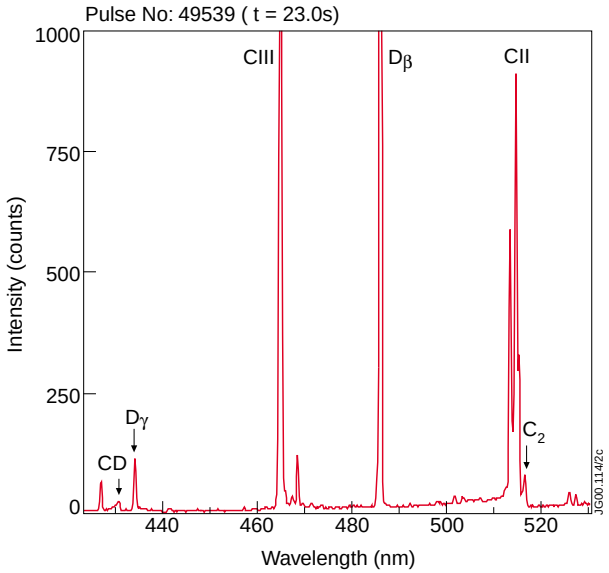

Fig.2: A portion of the KS3 spectrum from the outer divertor at 23.0s (i.e. high density, before the methane puff), showing the CD and C2 molecular band features.

The hydrocarbon gases were mostly injected through GIM 9 (slots in a toroidal ring in the floor of the outer divertor) rather than GIM 10 (in the sidewall of the outer divertor) because the spectroscopy has an un-vignetted view of GIM 9; see fig.1. The observed increases in molecular band intensities (ΔI_{puff}), compared with the intrinsic intensities ($I_{intrinsic}$) in deuterium/hydrogen puffed reference pulses, were used to deduce the intrinsic hydrocarbon influxes, $\Gamma_{intrinsic}$ ($\Gamma_{intrinsic} = \Gamma_{gas} * I_{intrinsic} / \Delta I_{puff}$) and erosion yields, Y ($Y = \Gamma_{intrinsic} / \Gamma_{D,H}$), as well as the D/XB ($D/XB = \Gamma_{gas} / \Delta I_{puff}$). Where Γ_{gas} is the flux of puffed hydrocarbon gas, and $\Gamma_{D,H}$ is the intrinsic deuterium influx calculated from either Langmuir probe measurements or the intrinsic deuterium intensity, $I_{D,H}$ ($\Gamma_{D,H} = I_{D,H} * S/XB$, where S/XB is the deuterium photon efficiency).

The assumption is made that the different source distributions (intrinsic vs. puffed) do not have a significant effect on the measurements. This assumption is supported by earlier measurements of D/XB in Elmy H-mode plasmas that found the same value whether the methane was injected into the private flux region (as here), or into the scrape-off-layer [5]. We also assume that the divertor cryopump does not pump a significant portion of the injected hydrocarbon gas, because the gas is directed vertically upwards towards the plasma edge and not towards the pumping slots at the junction between the horizontal and vertical divertor tiles.

2. RESULTS

The Scrape-off-Layer (SOL) plasma parameters in the outer divertor in typical 2.4MA, 2.5T L-mode discharges are shown in fig.3. For these plasmas the peak edge electron temperature (T_{ed}) was typically 20eV at low density, and 8eV at high density. The peak edge density (not shown) was more variable, but typically varied from $2x10^{19}$ m^{-3} to $1.5x10^{20}$ m^{-3}. The ratio of ion saturation current to the D-alpha intensity (the deuterium S/XB) was typically about 20 (fig.4), increasing slightly with density, indicating that the plasma in the outer divertor was always attached, as would be expected for these T_{ed}. In contrast, the inner divertor was only completely attached at the lowest plasma densities, as indicated in fig.4 by a fall in the derived S/XB ratio as the density increases.

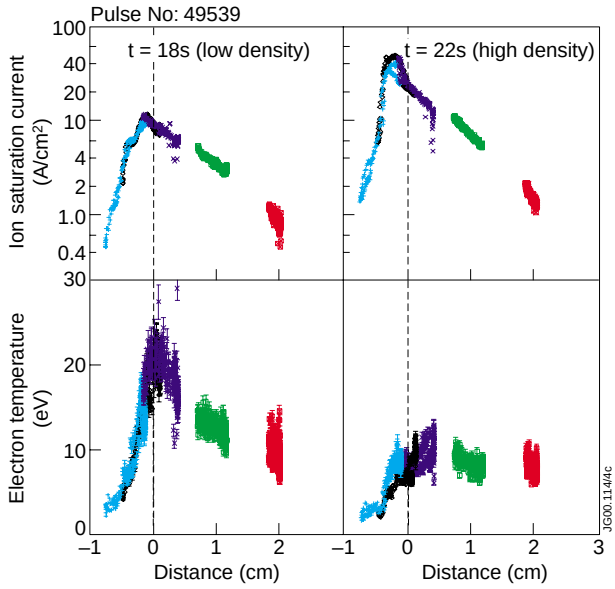

Fig.3: Ion saturation current and electron temperature profiles at the outer divertor target during the low and high density phases of these discharges. The distance scale is midplane centimetres relative to the separatrix.

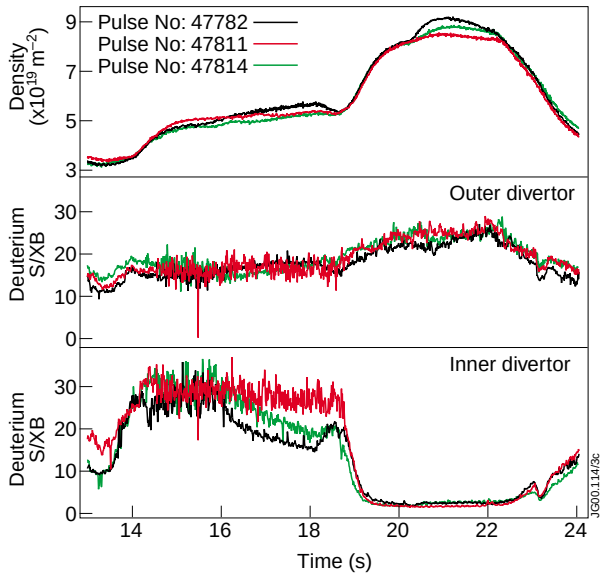

Fig.4: Density evolution as a function of time. Also shown is the D-alpha photon efficiency at the inner and outer divertor, calculated from the calibrated D-alpha signal and the integrated ion flux from the fixed Langmuir probes.

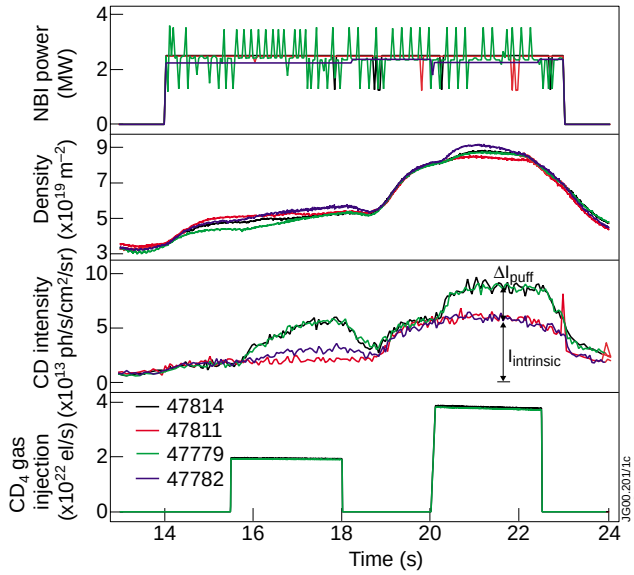

Fig.5: (a) The time evolution of the NB power, the central line integral density, the hydrocarbon puff rates and the outer divertor CD intensity for deuterium plasmas.

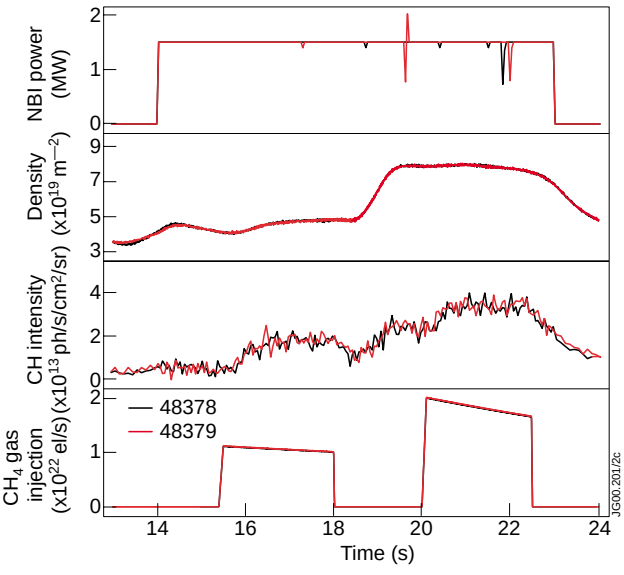

Fig.5: (b) The time evolution of the NB power, the central line integral density, the hydrocarbon puff rates and the outer divertor CH intensity for hydrogen plasmas.

Figure 5a shows data for CD_4 puffs into a deuterium plasma, and fig.5b for CH_4 puffs into a hydrogen plasma. The GIM 9 (outer divertor) hydrocarbon puffs in these discharges led to large increases in the CD (CH) molecular signals, and some increase in the signals from low charge states of carbon. However, the line-averaged Z_{eff} (typically 1.5) showed almost no change (ΔZ_{eff} <0.1). The figures illustrate that at high density twice as much methane injection was needed to achieve the same increase in CD (CH) signal as at low density. This implies that the

photon efficiency is higher at higher edge densities (lower edge temperatures). The figures also illustrate that (a) the intrinsic CD (CH) intensities are strongly density dependent, so reference discharges with a well-matched density are desirable, and (b) the intrinsic CD intensity in deuterium discharges is about twice as large as the intrinsic CH intensity in hydrogen discharges. This would suggest that the intrinsic erosion yield of CD_4 is twice that of CH_4, assuming that D/XB is isotope independent. Reference discharges were not available for the hydrogen plasmas in fig.5b, but by plotting the CH signal vs. density (fig.6) the intrinsic CH intensity can be estimated.

Ethane and ethene were also puffed from GIM 9 into 2.4MA, 2.5T ohmic hydrogen discharges (fig.7). Again it can be seen that twice as much gas needed to be puffed at high density in order to achieve the same increase in molecular C_2 intensity as at low density. It was also striking that the C_2 intensity was identical in the C_2H_4 and C_2H_6 puffed discharges, implying identical D/XB.

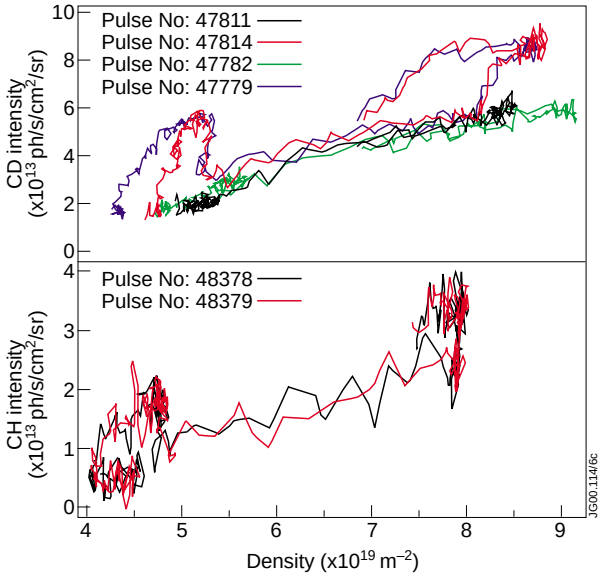

Fig.6: The evolution of CD (CH) intensities as a function of line integral density for deuterium (hydrogen) discharges with CD_4 (CH_4) puffing.

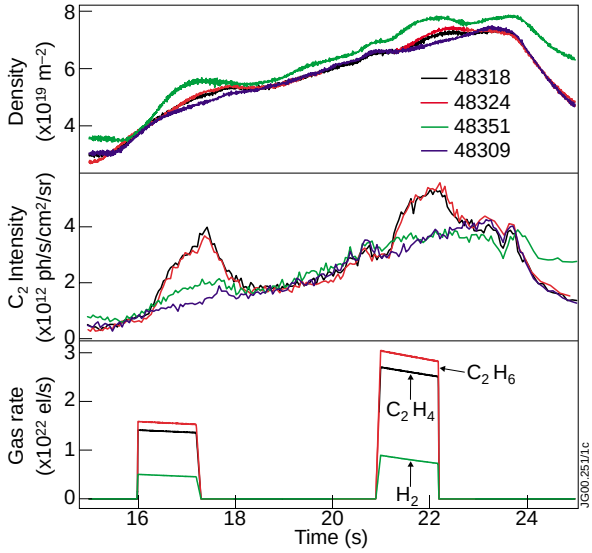

Fig.7: The time evolution of the central line integral density, C2 intensities and gas injection rates for hydrogen discharges with C_2H_4 or C_2H_6 gas puffing in the outer divertor.

There is the possibility that when the higher hydrocarbons are broken up in the plasma edge, significant fractions of CH are produced. If this were happening, then measurements of CH molecular band intensities would overestimate the methane source rate. Figure 8 shows that the CH intensity was possibly showing a small increase when C_2H_4 and C_2H_6 were puffed, although in another discharge no increase in inner divertor CH was seen for a strong inner divertor C_2H_4 puff. Thus we conclude that for our divertor plasma conditions the break-up of C_2H_y produces few CH molecules, though this is an area worthy of more detailed study.

The isotopic dependence of the methane D/XB was also explicitly investigated (fig.9). CD_4 was first puffed from GIM 9 into a 2.4MA, 2.5T ohmic deuterium plasma with a density ramp. The filling gas in GIM 9 was then changed to CH_4, and the discharge repeated. The

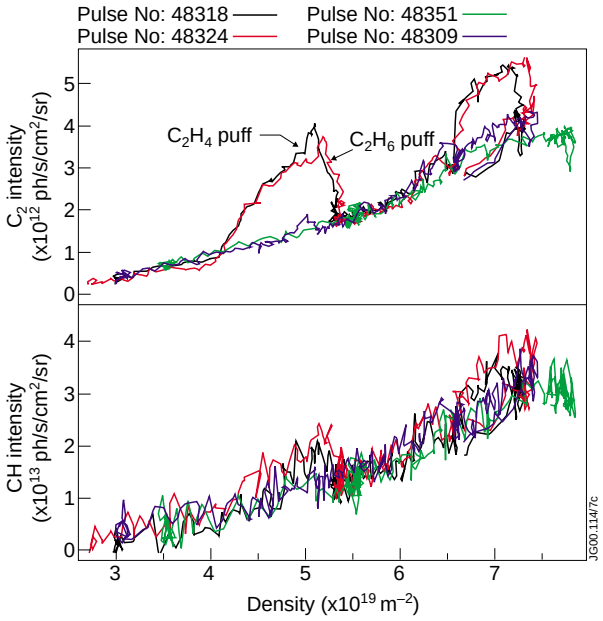

Fig.8: Evolution of C_2 and CH intensities as a function of line integral density for hydrogen discharges with C_2H_4 or C_2H_6 gas puffing in the outer divertor.

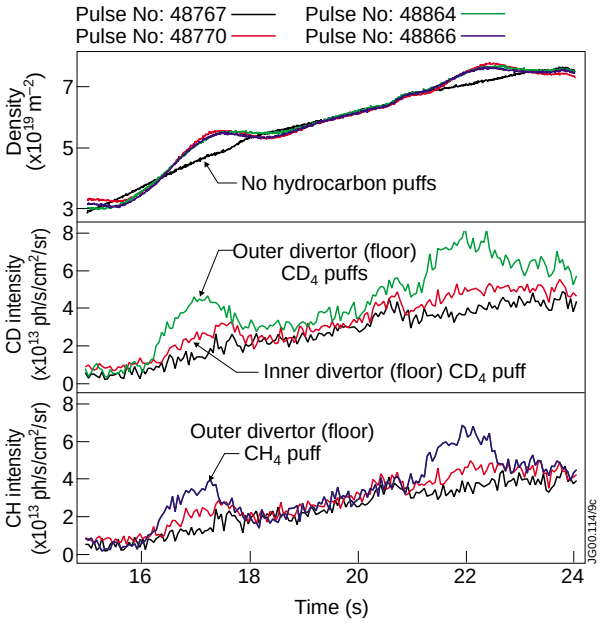

Fig.9: Time evolution of line integral density, outer divertor CD and CH intensities and gas injection rates for CD_4 and CH_4 gas puffing into similar deuterium target plasmas.

different methane isotopes were therefore puffed from the same location into the same edge plasma. The increases in the CD and CH intensities were found to be the same, within errors, and hence the methane D/XB was shown to be isotope independent.

Figures 10 and 11 show the full datasets for the hydrocarbon erosion yields and photon efficiencies. The erosion yields are all measurements from the outer divertor, except for a single point from the inner divertor, which will be discussed later. Each outer divertor erosion yield measurement in fig.10 is represented by two data points; one where the yield is calculated from an incident flux derived from the D-alpha measurement and a constant S/XB=20, the other where the yield is calculated from a total incident flux derived from the Langmuir probe signals. The probe measurements ought to be the more robust, but since there are not an infinite number of them the accuracy of the integral measurements depend critically on the relative location of the strike point relative to the probe positions. In the worst case, if the strike point were just missing a probe so that this nearest probe was in the private flux region, the total integrated ion flux would be significantly underestimated. This was probably the case for the C_2H_4 puff into a high density hydrogen plasma, where Y_{C2H4} = 5.5% from Langmuir probe data and Y_{C2H4} = 3.3% from D-alpha data (see data points in fig.10 at an integrated ion flux of 8.2×10^{22} s^{-1}).

Figure 10 shows that the methane erosion yields are constant; about 5% for deuterium plasmas and 3% for hydrogen plasmas, and do not show any flux dependence. In contrast, the erosion yield for C_2H_y (in hydrogen plasmas) does show an increase with the ion flux, rising from 1.8 to 3%. This means that at high density (i.e. high ion flux, or low electron temperature) in hydrogen plasmas the total carbon chemical erosion yield is three times the methane erosion

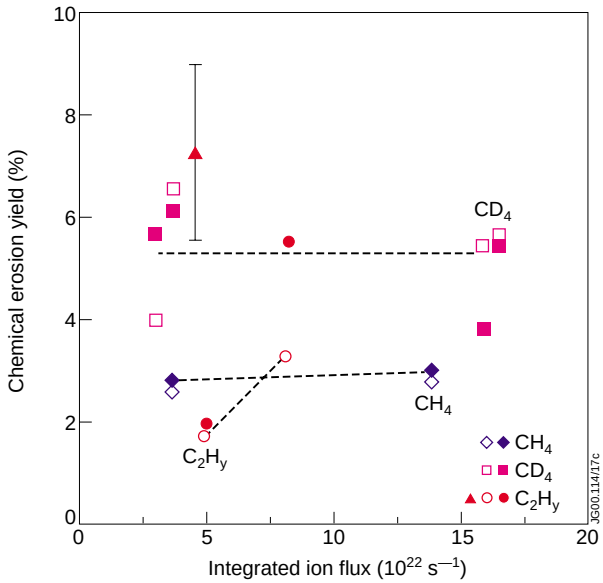

Fig.10: Hydrocarbon erosion yields as a function of the integrated ion flux to the outer divertor. The incident flux is calculated from Langmuir probe data for the solid data points, and from D-alpha (S/XB=20) for the open points. The ▲ is a C2H4 yield measurement from the inner divertor.

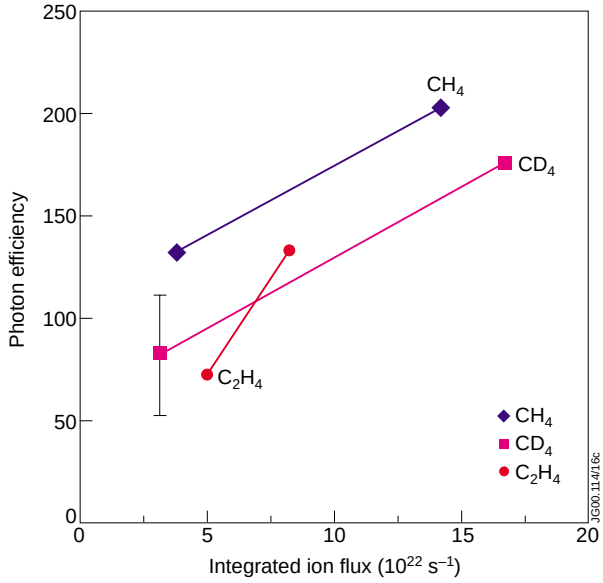

Fig.11: Hydrocarbon photon efficiencies as a function of the integrated ion flux to the outer divertor.

yield! If this factor is isotope independent, then the total carbon chemical erosion yield would be 15% in the outer divertor in deuterium plasmas.

Figure 10 also includes a data point for C_2H_4 injection into the inner divertor of a deuterium plasma. Assuming that the ethene D/XB is isotope independent, as found for methane, then its intrinsic erosion yield at the inner divertor is determined to be about 7%. Thus the total carbon chemical erosion yield at the inner divertor could be as high as 19%, assuming the same 5% CD_4 yield at the inner divertor as was measured in the outer divertor.

The photon efficiencies plotted in fig.11 show a strong increase with increasing ion flux. From our data it is not possible to determine whether the changes in photon efficiency are due to the changing ion flux, electron density, or electron temperature. In any case, these results are not consistent with the modelling of Naujoks [6], or the behaviour of the photon efficiencies of impurity ions, such as O II and C III, where photon efficiencies generally increase with increasing electron temperature and show little density dependence. Since the D/XB measurements are trying to relate the source molecule (e.g. C_2H_6) to photon emission from a molecular fragment (e.g. C_2) near the end of a complex dissociation chain, perhaps the dissociation reaction rates are inadequately known.

Earlier JET hydrocarbon yield data [4] had been analysed with the assumption of constant photon efficiency, and showed a decrease of the hydrocarbon yield with increasing flux density. If this earlier JET data is re-analysed using the CD_4 photon efficiencies from fig.11, and assuming a linear variation of D/XB with integrated ion flux, then the hydrocarbon yield becomes essentially

constant with increasing ion flux, figure 12. Other measurements that assumed a constant D/XB [2, 3], and which also showed decreasing erosion yield with increasing ion flux, would most likely show a similar effect.

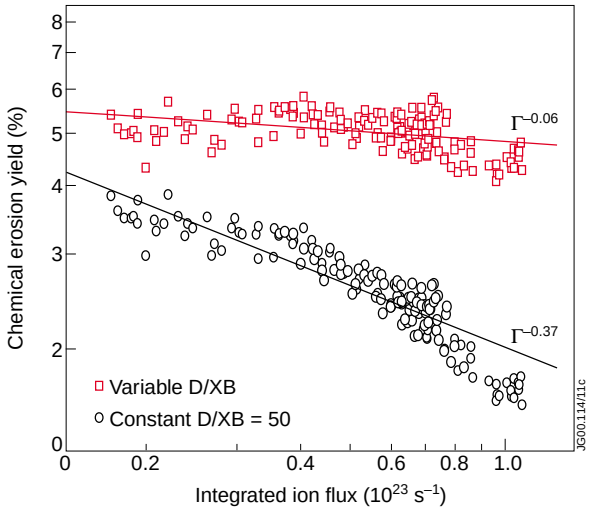

Fig.12: Revised plot of the chemical erosion yield data from [4] as a function of the integrated ion flux to the outer divertor, both for a constant D/XB (=50), and the measured variable D/XB.

3. SUMMARY

New measurements of the methane erosion yield in the JET Gas Box divertor found that it was a constant 5% for CD_4 in deuterium plasmas, and 3% for CH_4 in hydrogen plasmas. The recently reported flux dependence of the methane yield [2-4] was not observed, and seems to be a consequence of assuming a constant D/XB. Our measurements of D/XB (methane and ethane/ethene) show that D/XB increases strongly with increasing electron density or decreasing electron temperature.

The erosion yields of higher hydrocarbons were also measured and showed an unfavourable increase with ion flux, from 1.8% to 3% in hydrogen plasmas. Consequently, in hydrogen plasmas the total carbon chemical erosion yield was always at least double the methane yield. In a deuterium plasma, the ethene erosion yield was determined to be about 7% at the inner divertor. This is higher than the 3% maximum C_2H_y yield found at the outer divertor, and supports the hypothesis of readily eroded soft films that has been invoked to explain the thick carbon layers found on the inner louvers at JET [7].

It should be noted that these erosion yields are only the gross local yields. Net erosion yields will be much lower because these hydrocarbons are readily dissociated and ionised by the plasma and returned promptly to the divertor target plates. However, erosion yields of this magnitude, and the concomitant trapping of tritium in redeposited films, would present a tritium inventory problem for ITER [1], which might be alleviated by operating with the graphite at elevated temperatures (>600 K [8]).

4. ACKNOWLEDGEMENTS

The authors would like to thank L Horton and J Strachan for their support and for useful discussions.

This work is funded in part by the UK Department of Trade and Industry and Euratom, and was performed partly within the framework of the JET Joint Undertaking.

5. REFERENCES

[1] G Federici et al., J. Nucl. Mater. **266-269** (1999) 14.

[2] A Pospiezczyk et al., J. Nucl. Mater. **241-243** (1997) 833.

[3] A Kallenbach et al., Nucl. Fusion **38** (1998) 1097.

[4] R D Monk et al., Physica Scripta **T81** (1999) 54.

[5] M F Stamp et al., J Nucl. Mater. **266-269** (1999) 685.

[6] D Naujoks, D Coster, H Kastelewicz and R Schneider, J Nucl. Mater. **266-269** (1999) 360.

[7] P Coad et al., Proceedings of the 26th European Physical Society Conference on Controlled Fusion and Plasma Physics (Maastricht, Netherlands, 14th - 18th June 1999).

[8] J Roth, J Nucl. Mater. **266-269** (1999) 51.